PROCEEDINGS OF SCIENCE

Charged particle and underlying event measurements with the ATLAS detector[†]

Mustafa Schmidt[a,*] **on behalf of the ATLAS collaboration**

[a] *Bergische Universität Wuppertal,*
Gaußstraße 20, 42119 Wuppertal

E-mail: muschmidt@uni-wuppertal.de

Recent measurements by the ATLAS experiment are sensitive to the underlying event, the hadronic activity observed in relationship with the hard scattering in the event. Underlying event observables like the average particle multiplicity and the transverse momentum sum are measured for Kaons as Lambda baryons as a function of the leading track-jet and are compared to MC predictions which in general fail to describe the data. Furthermore, an analysis of the momentum differences between charged hadrons in proton-proton, proton-lead, and lead-lead collisions was conducted. The difference in the yield of hadron pairs with like-sign and opposite-sign charges is used to extract the spectra of pairs adjacent in color flow with the measurement being sensitive to the dynamics of hadronization.

*** ICHEP 2024 ***
*** 17-24 September 2024 ***
*** Pargue, Czech Republic ***

[*]Speaker

PoS(ICHEP2024)512

1. Introduction

Understanding the underlying event (UE) in proton-proton (pp) collisions and other hadronic systems is crucial for gaining insights into the dynamics of high-energy interactions. The UE includes all processes except for the direct products of the hard scatter and involves diffractive scattering, soft interactions, and hadronization. This document summarizes results from two different studies conducted with the ATLAS detector at the Large Hadron Collider (LHC): The first investigation focuses on underlying event characteristics in pp collisions at $\sqrt{s} = 13$ TeV, originating from $p\bar{p}$ results at CDF [1] and emphasizing strange hadron production. The second one examines ordered hadron chains in different collision systems (pp, $p + Pb$, $Pb + Pb$), exploring potential universal patterns in hadronization.

2. Underlying event studies with strange hadrons in pp collisions at $\sqrt{s} = 13$ TeV

2.1 Motivation

This study, presented in Ref. [2], focuses on the properties of the underlying event in pp collisions at $\sqrt{s} = 13$ TeV and examines the production of strange hadrons (K^0_S, Λ, $\bar{\Lambda}$). These hadrons are identified by their displaced vertices. The measured data was analyzed in different azimuth regions relative to the leading jet, as shown in Figure 1.

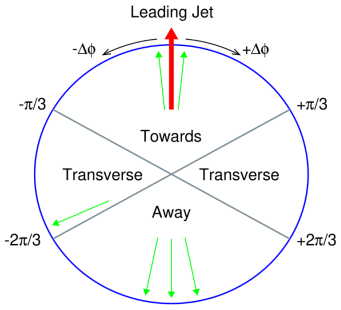

Figure 1: Illustration of the regions used in the underlying event studies [2].

The comparison of the results with predictions from various hadronization and UE physics models leads to an enhanced understanding of hadronization processes and multi-parton interactions (MPI). The data provided is also useful to improve and tune Monte Carlo (MC) simulation models.

2.2 Object and event selection

Prompt tracks, jets, and strange hadrons were selected using strict criteria as explained in the following. For prompt tracks with transverse and longitudinal impact parameters of ≤ 1.5 mm relative to the primary vertex, a selection cut of $p_T > 500$ MeV and $|\eta| < 2.5$ was used in addition to a maximum transverse impact parameter of 10 mm. Jets were reconstructed using the anti-k_t algorithm with a radius parameter $R = 0.4$ and a requirement for the highest-p_T (leading) jet within $|\eta| < 2.1$. An additional selection of large-radius tracks was applied using a secondary tracking step to improve efficiency for low-p_T particles and looser requirements on impact parameters with no

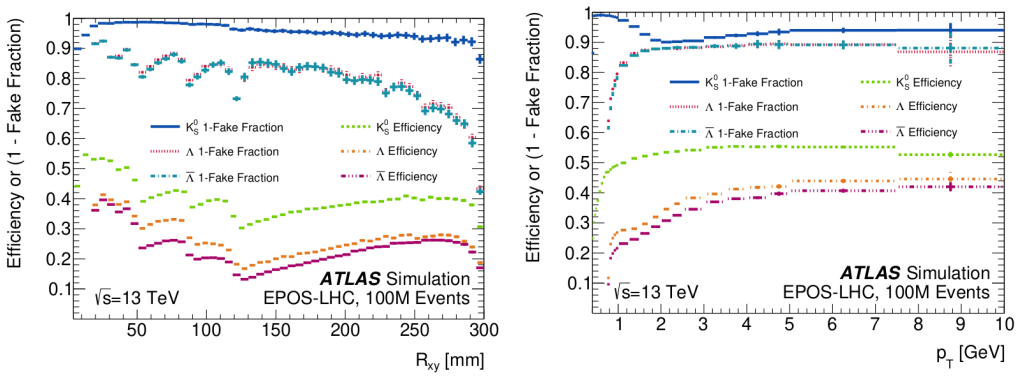

Figure 2: Correction factors for fake fractions and hadron efficiencies [2].

hit in the ATLAS pixel detector. A V^0-finder algorithm [3] was applied for K^0_S, Λ, and $\bar{\Lambda}$ candidates and events with constraints related to p_T thresholds, decay lengths, and mass windows.

The trigger requires at least one MBTS sector above the threshold for the single-hemisphere runs. Using a two-hemisphere trigger selection introduced a slight bias towards events with a larger number of charged particles. All events have to contain a primary vertex reconstructed from two or more tracks with $p_T > 100$ MeV, whereas pile-up events including two or more reconstructed primary vertices related to four or more associated tracks are removed. In addition, a transverse momentum window of $10 < p_T \leq 40$ GeV is applied to the leading jet. Regarding the track requirements, events must contain at least one track with $p_T > 1$ GeV passing prompt tracking selection, and particle-level events require at least one selected charged particle with $p_T > 1$ GeV. After applying all cuts including the strict leading-jet selection, 1.4 million events remain which are compared to a similar number of MC events.

2.3 Data and Monte-Carlo samples

In total, 130 million events were collected during the LHC run 2 in 2015 using single-hemisphere and double-hemisphere minimum bias trigger scintillators (MBTS) trigger conditions. During these runs, the mean number of inelastic interactions per bunch-crossing $\langle\mu\rangle$ varied between 0.003 and 0.03.

For the production of the MC samples, EPOS 3.4 with the EPOS-LHC tune [4] including parton-based Gribov-Regge theory was used. Furthermore, it includes Pythia 8 [5] with a special A2 tune, tuned using ATLAS minimum-bias data at 7 TeV, and a Monash and Color Reconnection (CR) tune. The latter includes an alternative CR model for improved baryon production. For all MC samples, trigger corrections were applied for the single-hemisphere MBTS trigger in addition to per-track and per-V^0 weights for correcting detector efficiencies and fake rates with mean correction factors for K^0_S, Λ, and $\overline{\Lambda}$ as shown in Figure 2.

2.4 Results

Three uncertainties were considered in this analysis. Unfolding uncertainties result from ratios between MC and data using the deviation of unfolded EPOS-LHC pseudo-data and Pythia 8 A2 response matrices. The fake V^0 probability has been obtained from line-shape fits taking the

material budget of the detector into account. And non-closure effects are related to the difference between reconstruction-level MC and particle-level distributions. The statistical uncertainties were calculated using bootstrap methods with 500 pseudo-runs.

Figure 3 shows two selected plots of the final results related to the normalized particle multiplicity as a function of the leading jet transverse momentum p_T. In the soft regime with a leading-jet $p_T < 10$ GeV, the EPOS-LHC model provided the best performance for K_S^0 and $\Lambda + \bar{\Lambda}$ mean multiplicities. However, it underestimated baryon yields at low p_T. Pythia 8 underestimates all distributions (up to 60% for $\Lambda + \bar{\Lambda}$), while the Monash+CR model performs slightly better than the A2 model, especially in the towards region for K_S^0 and $\Lambda + \overline{\Lambda}$ relative yields.

In the hard scattering regime with a leading-jet $p_T > 10$ GeV, a weaker dependence on leading-jet p_T was observed, because of non-diffractive pp interactions at low impact parameters dominating the observed activity. In the towards and away regions the results show a rising tendency for event-normalized mean multiplicity with increasing leading-jet p_T, whereas in the transverse region, a predominantly flat behavior over the hard regime is observed, minimally affected by leading partonic scattering. Overall, the EPOS LHC model is less accurate in the hard regime due to the lack of a hard-scattering model.

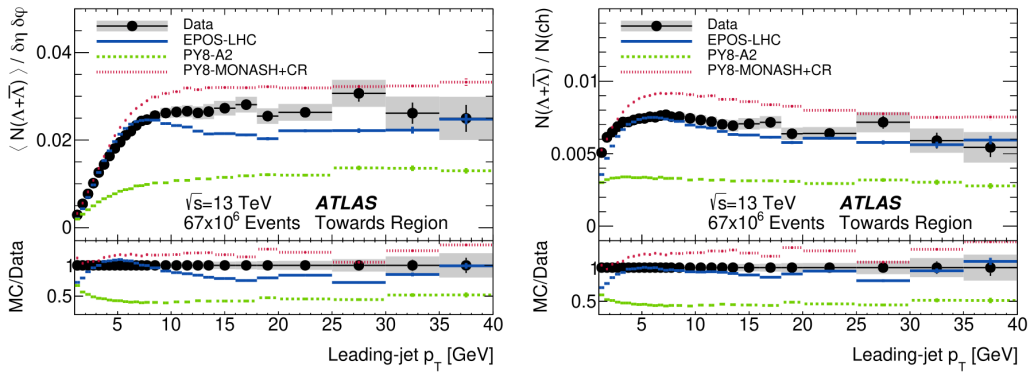

Figure 3: Results for $\Lambda + \bar{\Lambda}$ in the towards region [2].

3. Ordered hadron chains in pp, $p + Pb$, and $Pb + Pb$ collisions

3.1 Motivation

ATLAS offers a unique opportunity for momentum difference measurements between charged hadrons in different collision systems (pp, $p + Pb$, and $Pb + Pb$), exploring potential universal patterns in hadron production mechanisms [6]. Traditional models like the Lund string fragmentation model [7] still show discrepancies with experimental data. Hence, it is important to identify universal patterns in hadronization across different collision systems to get a deeper understanding of particle production mechanisms. Recent advancements in hadron physics propose a new helical string model [8] for hadronization which is part of this investigation. In this model, the important parameters are the hadron threshold m_{3h}^{thr} for three hadrons, the product κR of string tension and

helix radius, and the quantized helix phase $\Delta\phi$. The transverse energy $E_T(n)$ can then be written as

$$E_T(n) = \sqrt{m_n^2 + p_T(n)^2} = n\kappa R\Delta\phi \tag{1}$$

where n is the number of helical strings ($n = 1, 3, 5$) carrying portions of the transverse energy.

3.2 Methodology and results

The spectra of pair adjacent in color flow with a difference in hadron pair yield with like-sign (LS) and opposite-sign (OS) charges are extracted from the data. The differential charge distribution is defined as

$$\Delta(Q) = \frac{1}{N_{ch}}[N^{OS}(Q) - N^{LS}(Q)]$$

Furthermore, the following definitions of the correlation strength (CS) and the chain correlation strength (CCS) are required:

$$\mathrm{CS} = -\int_{\Delta<0} \Delta(Q)\,\mathrm{d}Q, \quad \mathrm{CCS} = -\int_{\Delta_{3h}<0} \Delta_{3h}(Q)\,\mathrm{d}Q$$

The study examines inclusive pair measurements, showing that $\Delta(Q)$ is independent of the collision energy, suggesting a universality in hadron production. The analysis of different systems revealed a rising correlation strength with the multiplicity, indicating a universal hadronization process (see the left side of Figure 4). It is the first LS pair production and model-independent measurement that can thus be used as a prediction for future minimum bias measurements.

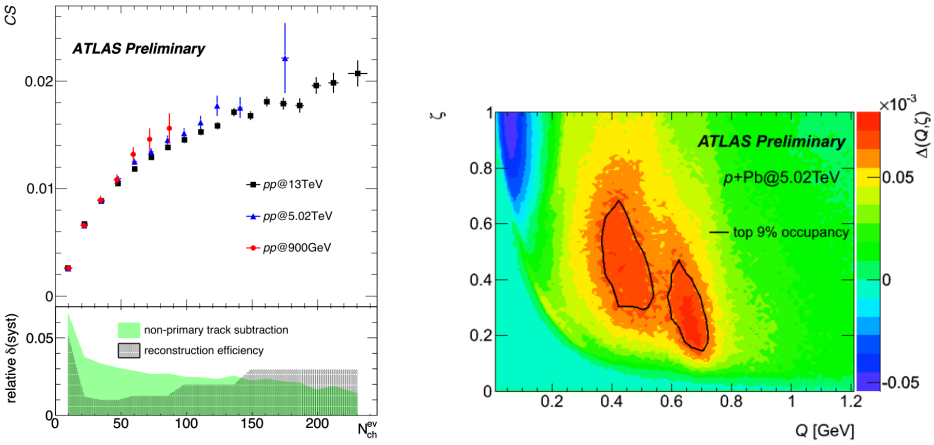

Figure 4: Inclusive pair measurements and universality of hadron productions across different collision systems [6].

The right side of Figure 4 illustrates the $\Delta(Q)$ distributions as a function of the ratio of absolute momenta

$$\zeta = \min\left(\frac{|p_j|}{|p_i|}, \frac{|p_j|}{|p_i|}\right)$$

and the momentum transfer Q. for the $p + Pb$ and $Pb + Pb$ systems which give direct insights into hadronization processes and identifying discrepancies in current models. This representation

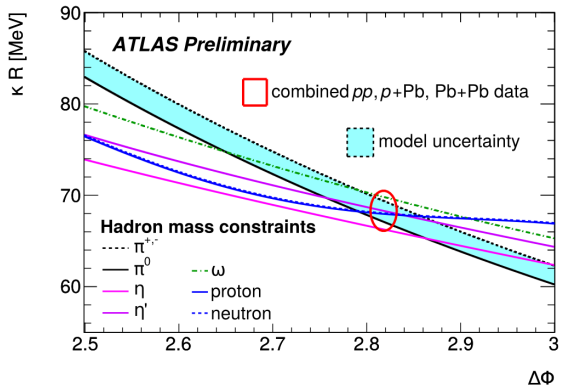

Figure 5: Hadron mass constraints for the helical string model [6].

allows a direct comparison of predictions from a MC generator based on the Hijing model [9] with experimental data. The black lines indicate areas where the model has to be improved further.

Finally, the results for all systems can be combined in a fit to calculate the parameters of the helical model:

$$m_{3h}^{thr} = (567^{+16}_{-19})\,\text{MeV}$$

$$\kappa r = (66.5^{+2.0}_{-2.2})\,\text{MeV}$$

$$\Delta\Phi = (2.819^{+0.013}_{-0.014})$$

Figure 5 shows an overview of the hadron mass constraints for the helical string model. The uncertainties include statical uncertainties as well as uncorrelated components of systematic uncertainties for fit stability and a threshold interpolation.

References

[1] CDF Collaboration, Phys. Rev. D **70** (2004) 072002.

[2] ATLAS Collaboration, arXiv:2405.05048 [hep-ex].

[3] ATLAS Collaboration, Phys. Rev. D **85** (2012) 012001.

[4] T. Pierog, I. Karpenko, J. M. Katzy, E. Yatsenko, and K. Werner, Phys. Rev. C **92** (2015) 034906.

[5] T. Sjöstrand et al., Comput. Phys. Commun. **191** (2015) 159.

[6] ATLAS Collaboration, ATLAS-CONF-2022-055, url: http://cds.cern.ch/record/2819852.

[7] S. Ferreres-Solé and T. Sjöstrand, Eur. Phys. J. C **78** (2018) 983.

[8] Š. Todorova-Nová, Phys. Rev. D **89** (2014) 015002.

[9] M. Gyulassy and X. Wang, Comput. Phys. Commun. **83** (1994) 307.